Available online at www.sciencedirect.com
SCIENCE DIRECT®
Tectonophysics 370 (2003) 129–145
TECTONOPHYSICS
www.elsevier.com/locate/tecto

Flow laws of multiphase materials and rocks from end-member flow laws

Shaocheng Ji[a,*], Pinglao Zhao[a], Bin Xia[b]

[a] *Département des Génies Civil, Géologique et des Mines, École Polytechnique de Montréal, C.P. 6079, Succursale Centre-Ville, Montréal, Québec, Canada H3C 3A7*

[b] *Guangzhou Institute of Geochemistry, Chinese Academy of Sciences, Wushan, Guangzhou, 510640, P.R. China*

Accepted 31 March 2003

Abstract

Rheological properties of polyphase rocks play an important role in the dynamics of the lithosphere and asthenosphere. However, flow laws for large portions of the polyphase rocks in the Earth's crust and mantle have not been well determined. An analysis based on the theory of mixtures has been made to calculate the general flow laws of coarse (≥ 5 μm), nearly equant-grained (aspect-ratio ≤ 3), and massive polyphase rocks and materials for which only the flow laws and volume fractions of the constituents are taken into consideration in the modeling of the bulk rheology and effects of microstructure could be ignored. The theoretical analysis is based on three assumptions: (1) the polyphase composite and the monophase aggregates of its constituents obey the same kind of flow laws (linear, power or exponential), (2) there is no change in the operative deformation mechanism of each phase when it is in the composite as compared to when it is in a monophase aggregate, and (3) neither chemical (metamorphic) reactions take place among the constituent phases nor eutectic melting occurs due to the phase mixing. The proposed iterative process allows to predict, to the first approximation, the flow laws for a large number of polyphase rocks in terms of the experimentally determined flow laws of a relatively small number of monomineralic aggregates. Applications of this approach to typical polyphase rocks such as granite, diorite, diabase, aplite and websterite as well as to synthetic two-phase materials such as forsterite–enstatite mixtures and water ice–ammonia dehydrate aggregates yield quite accurate approximations to the experimental values.

Keywords: Polyphase materials; Polyphase rocks; Flow law; Rheology; Deformation; Rules of mixture

1. Introduction

Constitutive laws used to describe steady-state flow behavior for both monophase and polyphase materials deformed by intracrystalline plastic flow are generally assumed to have a power law stress dependency and are of the form (Carter and Tsenn, 1987; Rutter and Brodie, 1992; Kohlstedt et al., 1995):

$$\dot{\varepsilon} = Ad^{-m}\sigma^{n}\exp\left(\frac{-Q}{RT}\right) \quad (1)$$

where $\dot{\varepsilon}$ is the steady-state strain-rate, A is the pre-exponential factor, σ is the differential flow stress, n is the stress exponent, Q is the apparent activation

* Corresponding author. Fax: +1-514-3403970.
E-mail address: sji@polymtl.ca (S. Ji).

0040-1951/03/$ - see front matter © 2003 Elsevier B.V. All rights reserved.
doi:10.1016/S0040-1951(03)00182-3

energy, R is the gas constant, T is the absolute temperature (K), d is the grain size and m is the grain size exponent.

At low stresses or at very high temperatures or under hydrous conditions, it is generally believed that plastic flow is dominated by diffusion creep (e.g., Rutter, 1976; Poirier, 1985). The materials behave as Newtonian fluids with strain-rate linearly related to stress (i.e., $n=1$). Deformation takes place by the actual transfer of vacancies from the surface of low compressive stress to the surface of high compressive stress. Vacancies are created at the surface of low compressive stress and flow either through the crystal lattice (so-called Nabarro-Herring creep and $m=2$) or along grain boundaries (Coble creep and $m=3$) to the surface of high compressive stress. The flux of material is opposite to that of the vacancies. Usually, Coble creep is effective at lower temperatures than Nabarro-Herring creep because of its lower activation energy. In the regime of diffusion creep, the flow strength tends to decrease rapidly with decreasing grain size (e.g., Karato et al., 1986; Walker et al., 1990; Bruhn et al., 1999; Rybacki and Dresen, 2000).

At the intermediate stress and temperature regime, flow is controlled by the mechanism of dislocation creep and is independent on the grain size (i.e., $m=0$). One model for the mechanism of dislocation creep, known as Weertman creep, assumes that the rate of dislocation glide is limited by the rate at which dislocations can climb. For Weertman creep, the value of stress exponent n is between 2 and 5 (e.g., Poirier, 1985; Walker et al., 1990; Mackwell et al., 1998; Rybacki and Dresen, 2000). It is also called power law flow, which is the dominant mechanism for most metamorphic conditions in the crust and upper mantle.

At high stress level, the strain-rate for plastic deformation increases approximately exponentially with increasing differential stress and the power flow law breaks down (Tsenn and Carter, 1987). The deformation is controlled by glide of dislocations through the lattice. Resistance to the motion of the dislocations comes in part from the lattice itself because of the necessity of breaking bonds in order for the dislocations to move. Resistance also comes from obstacles that occur in the path of a gliding dislocation, such as other dislocations or impurities. The stress dependence of the strain-rate is given by Tsenn and Carter (1987):

$$\dot{\varepsilon} = A\exp\left(\frac{-Q}{RT}\right)\exp(\beta\sigma) \tag{2}$$

where β is a constant for the flow in this high stress regime.

Flow laws, volume fractions and microstructures (e.g., shape, continuity and interconnectivity) of the constituent phases are generally considered as the most important factors controlling the bulk rheological properties of polyphase materials and rocks (e.g., Burg and Wilson, 1987; Ross et al., 1987; Jordan, 1988; Bloomfield and Covey-Crump, 1993; Handy, 1994; Ji and Zhao, 1994; Tullis and Wenk, 1994; Zhao and Ji, 1997; Dresen et al., 1998; Ji et al., 2000; McDonnell et al., 2000; Treagus, 2002). Because microstructures are complex and very rich in details, it is difficult to obtain an exact analytical solution to describe their effects on the nonlinear rheology of polyphase aggregates. The technique currently used for such studies is finite element modeling as made by Tullis et al. (1991), Dragone and Nix (1990) and Park and Holmes (1992). However, as pointed out by Tullis et al. (1991), the finite element modeling is too tedious to employ for each new aggregate because each polyphase material has a distinct microstructure. The results from such a modeling sometimes is so complicated that it might obscure the problem at hand. This study addresses the less troublesome case of coarse ($\geq 5\mu m$), nearly equant-grained (aspect-ratio ≤ 3), and massive rocks and materials for which we can take only the flow laws and volume fractions of the constituent phases into consideration and neglect the effects of microstructure. In this paper, we introduce a simple method for calculating the flow laws of such polyphase materials from their monophase flow laws and modal compositions.

Ji and Zhao (1993) developed an iterative model based on the geometric average of strain-rate or stress on $\dot{\varepsilon}$–σ coordinate system to directly determine the bulk flow law parameters (n, A, Q) of polyphase materials deforming in the regime of dislocation creep ($m=0$, the grain-size insensitive flow) in terms of the volume fractions and dislocation creep power law parameters of the constituent phases. In this paper, we will extend the iterative model of Ji and Zhao

(1993) to polyphase composites deformed by either dislocation creep (grain-size insensitive) or diffusion creep (grain-size sensitive), as long as deformation mechanism of each phase does not change when in the composite as compared to when it is in a single phase aggregate. This generalized model allows one to predict the flow laws of a large number of polyphase rocks at both laboratory and geological conditions based on the experimentally determined flow laws of a relatively small number of monophase aggregates.

2. Power law flow

2.1. Rules of mixture

There are two basic rules of mixture widely used in the material sciences and rock mechanics for predicting the bulk mechanical properties of composites (Kelly and Macmillan, 1986) and polyphase rocks (Watt et al., 1976; Tullis et al., 1991; Ji and Wang, 1999). These are:

(1) Uniform strain average, which suggests that the overall stress in the composite is equal to the arithmetic weight average of the stresses in the constituent phases and the weight factors are the volume fractions of the phases, but the strain or strain-rate is uniform in the composite.
(2) Uniform stress average, which suggests that the overall strain is equal to the arithmetic weight average of the strains in the phases and the stress is uniform in the composite.

Under these end-member conditions, the bulk stress (σ_c) and strain rate ($\dot{\varepsilon}_c$) of the composite can be represented by those of its constituent phases as follows:

$$\sigma_c^v = \sum_{i=1}^{N} V_i \sigma_i \tag{3}$$

$$\dot{\varepsilon}_c^r = \sum_{i=1}^{N} V_i \dot{\varepsilon}_i \tag{4}$$

where V represents the volume fraction and N is the number of constituent phases. The subscripts c and i stand for the composite and ith constituent phase, respectively. The superscripts r and v stand for the uniform stress average and uniform strain average, respectively. In the regime of elastic deformation, the uniform stress average and uniform strain average correspond, respectively, to the Reuss (1929) and Voigt (1928) bounds. The uniform strain average is assumed to be valid only when the constituent phases are continuous in the loading direction and if the mechanical interaction between the phases is neglected. On the other hand, the uniform stress average is assumed to be valid only when the constituent phases form continuous layers perpendicular to the loading direction and if there is no mechanical interaction between the phases (see Ji et al., 2000 for discussion). For the granular composites discussed in this paper, Eqs. (3) and (4) are believed to provide the upper and lower bounds to the flow strength of composite but not the real value (Tullis et al., 1991).

One important consequence of the application of these rules of mixture is that the resultant composite creep data cannot be represented by a simple power flow law although the relation between flow stress and strain-rate for each phase follows a power flow law. To solve this problem, Ji and Zhao (1993) proposed to use a geometric average rather than an arithmetic average of strain-rate or flow stress. On a $\ln \dot{\varepsilon}$–$\ln \sigma$ coordinate system (Fig. 1), Eq. (1) is represented as a straight line with a slope equal to n_i and an intercept equal to ($\ln A_i - m_i \ln d_i - Q_i/RT$). Corresponding to the N phases in the aggregate, there are N straight

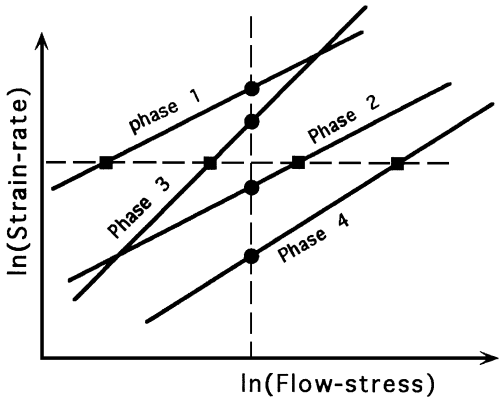

Fig. 1. Schematic representation of geometrical averaging methods for isostrain-rate and isostress conditions. Dot: isostress condition. Square: isostrain-rate condition.

lines on the plot. The geometric average on the $\dot{\varepsilon}$–σ coordinate system is then replaced by an arithmetic average on the $\dot{\varepsilon}$–ln σ coordinate system.

On the ln $\dot{\varepsilon}$–ln σ coordinate system, the power flow law equation for the ith phase in a polyphase aggregate containing N phases can be written as

$$\ln\dot{\varepsilon}_i = \ln A_i + n_i \ln\sigma_i - m_i \ln d_i - \frac{Q_i}{RT} \quad (i = 1,\ 2,\ \ldots,\ N) \tag{5}$$

or

$$\ln\sigma_i = \frac{1}{n_1}\left(\ln\dot{\varepsilon}_i - \ln A_i + m_i \ln d_i + \frac{Q_i}{RT}\right) \quad (i = 1,\ 2,\ \ldots,\ N) \tag{6}$$

where $\dot{\varepsilon}_i$ and σ_i are, respectively, the average strain-rate and average flow stress in the ith phase, (n_i, m_i, A_i, Q_i) are the flow law parameters of the ith phase and d_i is the grain size of the ith phase. If the polyphase aggregate obeys the same kind of constitutive flow laws as its constituent phases do, the composite flow law can be similarly written as

$$\ln\dot{\varepsilon}_c = \ln A_c + n_c \ln\sigma_c - m_c \ln d_c - \frac{Q_c}{RT} \tag{7}$$

or

$$\ln\sigma_c = \frac{1}{n_c}\left(\ln\dot{\varepsilon}_c - \ln A_c + m_c \ln d_c + \frac{Q_c}{RT}\right) \tag{8}$$

where d_c is the average grain size for the composite, as defined by Wang (1994), although its physical meaning has not been clear yet.

$$d_c = \sum_{i=1}^{N} V_i d_i \tag{9}$$

where V_i is the volume fraction of the ith phase. Eq. (9) can be rewritten as:

$$d_i = \frac{d_i}{\sum_{j=1}^{N} V_j d_j} d_c = \alpha_i d_c \qquad (i = 1,\ 2,\ \ldots,\ N) \tag{10}$$

where α_i is a constant.

By assuming uniform stress or uniform strain-rate in the polyphase aggregate, the overall strain-rate or the bulk flow stress of the polyphase aggregate can be respectively represented as

$$\ln\dot{\varepsilon} = \sum_{i=1}^{N} V_i \ln\dot{\varepsilon}_i = \sum_{i=1}^{N} V_i \ln A_i + \ln\sigma \sum_{i=1}^{N} V_i n_i - \sum_{i=1}^{N} V_i m_i \ln d_i - \frac{1}{RT}\sum_{i=1}^{N} V_i Q_i \tag{11}$$

and

$$\ln\sigma = \sum_{i=1}^{N} V_i \ln\sigma_i = \ln\dot{\varepsilon}\sum_{i=1}^{N}\frac{V_i}{n_i} + \sum_{i=1}^{N}\frac{V_i m_i}{n_i}\ln d_i - \sum_{i=1}^{N}\frac{V_i}{n_i}\ln A_i + \frac{1}{RT}\sum_{i=1}^{N}\frac{V_i}{n_i} Q_i \tag{12}$$

Substituting Eq. (10) into Eqs. (11) and (12), we obtain

$$\ln\dot{\varepsilon} = \sum_{i=1}^{N} V_i \ln A_i - \sum_{i=1}^{N} V_i m_i \ln\alpha_i + \ln\sigma \sum_{i=1}^{N} V_i n_i - \ln d_c \sum_{i=1}^{N} V_i m_i - \frac{1}{RT}\sum_{i=1}^{N} V_i Q_i \tag{13}$$

and

$$\ln\sigma = \ln\dot{\varepsilon}\sum_{i=1}^{N}\frac{V_i}{n_i} + \sum_{i=1}^{N}\frac{V_i m_i}{n_i}\ln\alpha_i - \sum_{i=1}^{N}\frac{V_i}{n_i}\ln A_i + \ln d_c \sum_{i=1}^{N}\frac{V_i m_i}{n_i} + \frac{1}{RT}\sum_{i=1}^{N}\frac{V_i}{n_i} Q_i \tag{14}$$

By comparing Eqs. (13) and (14) with Eqs. (7) and (8), respectively, we can obtain the flow law parameters for the polyphase aggregate by the uniform stress and uniform strain-rate averages on the ln $\dot{\varepsilon}$–ln σ plot:

$$n_c^r = \sum_{i=1}^{N} V_i n_i \tag{15}$$

$$m_c^r = \sum_{i=1}^{N} V_i m_i \tag{16}$$

$$A_c^r = \prod_{i=1}^{N} \left(\frac{A_i}{\alpha_i^{m_i}} \right)^{V_i} \tag{17}$$

$$Q_c^r = \sum_{i=1}^{N} V_i Q_i \tag{18}$$

and

$$n_c^v = \frac{1}{\sum_{i=1}^{N} \frac{V_i}{n_i}} \tag{19}$$

$$m_c^v = n_c^v \sum_{i=1}^{N} \frac{V_i m_i}{n_i} \tag{20}$$

$$A_c^v = \prod_{i=1}^{N} \left(\frac{A_i}{\alpha_i^{m_i}} \right)^{n_c^v V_i / n_i} \tag{21}$$

$$Q_c^v = n_c^v \sum_{i=1}^{N} \frac{V_i Q_i}{n_i} \tag{22}$$

where the superscripts r and v stand for the uniform stress and uniform strain-rate approximations, respectively.

2.2. Iterative process

Neither the uniform stress nor uniform strain-rate is physically realistic (Tullis et al., 1991); therefore, the flow law in the real case should lie somewhere between the uniform stress and the uniform strain-rate averages. Following this concept, Ji and Zhao (1993) proposed a method to determine the approximate values of the flow law parameters of the dislocation-creep power law for polyphase rocks by taking these two averages as new input data and processing an iterative process to progressively reduce the range between the new averages until a given precision (B) is reached. A process is presented below to determine the flow law parameters for the general power law described by Eq. (1) by taking Eqs. (13) and (14) as two end-member flow laws:

$$n_{r(0)} = n_c^r \tag{23}$$

$$m_{r(0)} = m_c^r \tag{24}$$

$$A_{r(0)} = A_c^r \tag{25}$$

$$Q_{r(0)} = Q_c^r \tag{26}$$

$$n_{v(0)} = n_c^v \tag{27}$$

$$m_{v(0)} = m_c^v \tag{28}$$

$$A_{v(0)} = A_c^v \tag{29}$$

$$Q_{v(0)} = Q_c^v \tag{30}$$

Then the iterative process can be realized according to the following equations

$$n_{r(i)} = F n_{v(i-1)} + (1-F) n_{r(i-1)} \tag{31}$$

$$m_{r(i)} = F m_{v(i-1)} + (1-F) m_{r(i-1)} \tag{32}$$

$$A_{r(i)} = (A_{v(i-1)})^F (A_{r(i-1)})^{1-F} \tag{33}$$

$$Q_{r(1)} = F Q_{v(i-1)} + (1-F) Q_{r(i-1)} \tag{34}$$

for the uniform stress approximation of the fictitious "two-phase" aggregate (new "lower bound"), and

$$n_{v(i)} = \frac{n_{v(i-1)} n_{r(i-1)}}{(1-F) n_{v(i-1)} + F n_{r(i-1)}} \tag{35}$$

$$m_{v(i)} = \frac{F n_{r(i-1)} m_{v(i-1)} + (1-F) n_{v(i-1)} m_{r(i-1)}}{n_{v(i-1)} n_{r(i-1)}} n_{v(i)} \tag{36}$$

$$A_{v(i)} = \left(A_{v(i-1)}\right)^{Fn_{v(i)}/n_{v(i-1)}} \left(A_{r(i-1)}\right)^{(1-F)n_{v(i)}/n_{r(i-1)}} \quad (37)$$

$$Q_{v(i)} = \frac{Fn_{r(i-1)}Q_{v(i-1)} + (1-F)n_{v(i-1)}Q_{r(i-1)}}{n_{v(i-1)}n_{r(i-1)}} n_{v(i)} \quad (38)$$

for the uniform strain-rate approximation of the fictitious "two-phase" aggregate (new "upper bound").

Here F is a coefficient to describe the contribution of the uniform strain-rate condition. Its value depends on the microstructure of the material. When the loading direction is parallel to the layering of a layered composite, in which different constituent phases form different layers, the composite is deformed in uniform strain-rate and $F=1$. On the other hand, when the loading direction is normal to the layers, the composite is deformed in uniform stress and thus $F=0$. For a granular rock, the value of F is between 0 and 1. It is found that $F=0.5$, where the uniform stress and uniform strain conditions have equal contributions, yields the best agreement between the theoretically calculated and experimentally measured flow strengths for polyphase materials. For a given precision (B), the iterative process will continue until the following conditions are satisfied

$$\frac{|n_{v(s)} - n_{r(s)}|}{(n_{v(s)} + n_{r(s)})} < B, \quad \frac{|m_{v(s)} - m_{r(s)}|}{(m_{v(s)} + m_{r(s)})} < B,$$

$$\frac{|A_{v(s)} - A_{r(s)}|}{(A_{v(s)} + A_{r(s)})} < B, \text{ and } \frac{|Q_{v(s)} - Q_{r(s)}|}{(Q_{v(s)} + Q_{r(s)})} < B \quad (39)$$

where s is the number of iterative steps needed to reach the precision B (e.g., $B=1\%$). Finally, either the "lower bound" parameters ($n_{r(s)}$, $m_{r(s)}$, $A_{r(s)}$, $Q_{r(s)}$) or the "upper bound" parameters ($n_{v(s)}$, $m_{v(s)}$, $A_{v(s)}$, $Q_{v(s)}$) can be taken as the flow law parameters for the polyphase aggregate because the difference between these two "bounds" can be ignored.

To realize the above iterative process, a QuickBasic program has been written and is available upon request from the authors.

3. Exponential law flow

At high stress level, the strain-rate of steady-state flow becomes increasingly sensitive to differential stress as the differential stress increases. If one attempts to explain the experimental data with the power law described by Eq. (1), one will find that the stress exponent n increases with increasing differential stress. It has been found that an exponential dependence of strain-rate upon differential stress, named exponential law (Eq. (2)), best describes the experimental data (Sherby et al., 1954; Tsenn and Carter, 1987).

The exponential law (Eq. (2)), can be transferred into a linear relationship on $\ln\dot{\varepsilon}$–$\ln\sigma$ coordinate system.

$$\ln\dot{\varepsilon} = \ln A - \frac{Q}{RT} + \beta\sigma \quad (40)$$

Repeating the similar process described in Section 2.2, we can obtain the following equations to calculate, respectively, the exponential law parameters of the "lower and upper bounds" with the uniform stress and uniform strain-rate approximations for a given polyphase material consisting of N phases.

$$\beta_c^r = \sum_{i=1}^{N} V_i\beta_i \quad (41)$$

$$A_c^r = \prod_{i=1}^{N} A_i^{V_i} \quad (42)$$

$$Q_c^r = \sum_{i=1}^{N} V_iQ_i \quad (43)$$

and

$$\beta_c^v = \frac{1}{\sum_{i=1}^{N} \frac{V_i}{\beta_i}} \quad (44)$$

$$A_c^v = \prod_{i=1}^{N} A_i^{V_i\beta_c^v/\beta_i} \quad (45)$$

$$Q_c^v = \beta_c^v \sum_{i=1}^{N} \frac{V_iQ_i}{\beta_i} \quad (46)$$

By taking the exponential law parameters in Eqs. (41)–(43) and (44)–(46) as two new end-member flow laws,

$$\beta_{r(0)} = \beta_c^r \tag{47}$$

$$A_{r(0)} = A_c^r \tag{48}$$

$$Q_{r(0)} = Q_c^r \tag{49}$$

and

$$\beta_{v(0)} = \beta_c^v \tag{50}$$

$$A_{v(0)} = A_c^v \tag{51}$$

$$Q_{v(0)} = Q_c^v, \tag{52}$$

the iterative process used for calculating the new approximate exponential law parameters can be realized by considering

$$\beta_{r(i)} = F\beta_{v(i-1)} + (1-F)\beta_{r(i-1)} \tag{53}$$

$$A_{r(i)} = (A_{v(i-1)})^F (A_{r(i-1)})^{1-F} \tag{54}$$

$$Q_{r(i)} = FQ_{v(i-1)} + (1-F)Q_{r(i-1)} \tag{55}$$

and

$$\beta_{v(i)} = \frac{\beta_{v(i-1)}\beta_{r(i-1)}}{(1-F)\beta_{v(i-1)} + F\beta_{r(i-1)}} \tag{56}$$

$$A_{v(i)} = (A_{v(i-1)})^{F\beta_{v(i)}/\beta_{v(i-1)}} (A_{r(i-1)})^{(1-F)\beta_{v(i)}/\beta_{r(i-1)}} \tag{57}$$

$$Q_{v(i)} = \frac{F\beta_{r(i-1)}Q_{v(i-1)} + (1-F)\beta_{v(i-1)}Q_{r(i-1)}}{\beta_{v(i-1)}\beta_{r(i-1)}}\beta_{v(i)} \tag{58}$$

After s steps of iteration, the difference between the new "lower and upper bounds" will be less than a given precision (B). Then, either the "lower bound" parameters ($\beta_{r(s)}$, $A_{r(s)}$, $Q_{r(s)}$) or the "upper bound" parameters ($\beta_{v(s)}$, $A_{v(s)}$, $Q_{v(s)}$) can be taken as the approximate exponential law parameters for the polyphase material because the difference between these two "bounds" can be ignored when B is small enough ($<1\%$).

4. Prediction of flow law parameters for monophase rocks

The major purpose of this study is to estimate the flow law parameters of polyphase materials in terms of the flow laws and volume fractions of their constituent phases. Occasionally, one may be interested in a reversed problem, that is, estimation of the flow law parameters of a monophase aggregate which is one of

Table 1
Predicted flow law parameters for typical polyphase rocks and input data

Rock	Composition for modeling	A (MPa^{-n}/s)	n	Q (kJ/mol)	Reference
Diorite	Rock	1.26×10^{-3}	2.4	219	[1]
	66% pl	3.27×10^{-4}	3.2	238	[2]
	28% cpx (hb)	15.8	2.6	335	[2]
	6% qtz	10^{-3}	2.0	167	[2]
	Prediction	8.7×10^{-3}	2.93	261.5	This study
Diabase	Rock	2.0×10^{-4}	3.4	260	[2]
	64% cpx	1.58×10^{-5}	6.4	444	[3]
	36% pl	3.27×10^{-4}	3.2	238	[2]
	Prediction	6.12×10^{-5}	4.97	351.9	This study
	Prediction	6.02×10^{-5}	4.99	353.0	[7]
Granite	Rock	2.0×10^{-6}	3.3	187	[1]
	Rock	2.6×10^{-9}	3.4	138	[1]
	68% pl	2.34×10^{-6}	3.9	234	[2]
	27% qtz	10^{-3}	2	167	[2]
	5% bi	1.3×10^{-67}	31	98	[4]
	Prediction	5.74×10^{-7}	3.90	206.4	This study
Aplite	Rock	3.26×10^{-7}	3.1	163	[2]
	65% pl	2.34×10^{-6}	3.9	234	[2]
	30% qtz	10^{-3}	2	167	[2]
	5% bi	1.3×10^{-67}	31	98	[5]
	Prediction	7.18×10^{-7}	3.84	204.2	This study
Websterite	Rock	3.98×10^{-7}	4.3	326	[5]
	68% cpx	10^{-5}	5.3	380	[3]
	32% opx	0.316	2.4	293	[6]
	Prediction	7.6×10^{-4}	4.09	343.6	This study
	Prediction	6.94×10^{-4}	4.11	344.4	[7]

[1] Hansen and Carter (1982); [2] Shelton and Tullis (1981); [3] Kirby and Kronenberg (1984); [4] Shea and Kronenberg (1992); [5] Avé Lallemant (1978); [6] Raleigh et al. (1971); [7] Tullis et al. (1991).

Abbreviations: bi = biotite, cpx = clinopyroxene, hb = hornblende, ol = olivine, opx = orthopyroxene, pl = plagioclase, qtz = quartz.

the constituent phases of a polyphase material. If the flow law parameters of this polyphase material and its other constituent phases are known, the flow law parameters of this phase can then be calculated from the present model by the following variable transfers.

(1) Taking the unknown phase as a "polyphase material" while the polyphase material as the last phase [i.e., the Nth phase in Eqs. (5) and (6)].
(2) The volume fraction values for the first $N-1$ phases are taken as the reserved values (i.e., negative values) of their real volume fractions. The volume fraction for the Nth phase (i.e., the real polyphase material) is taken as 1.

5. Applications to polyphase rocks

In the following, we will show some examples for the application of the methods to polyphase rocks. The flow law parameters of monophase aggregates used as input data to predict the flow law parameters

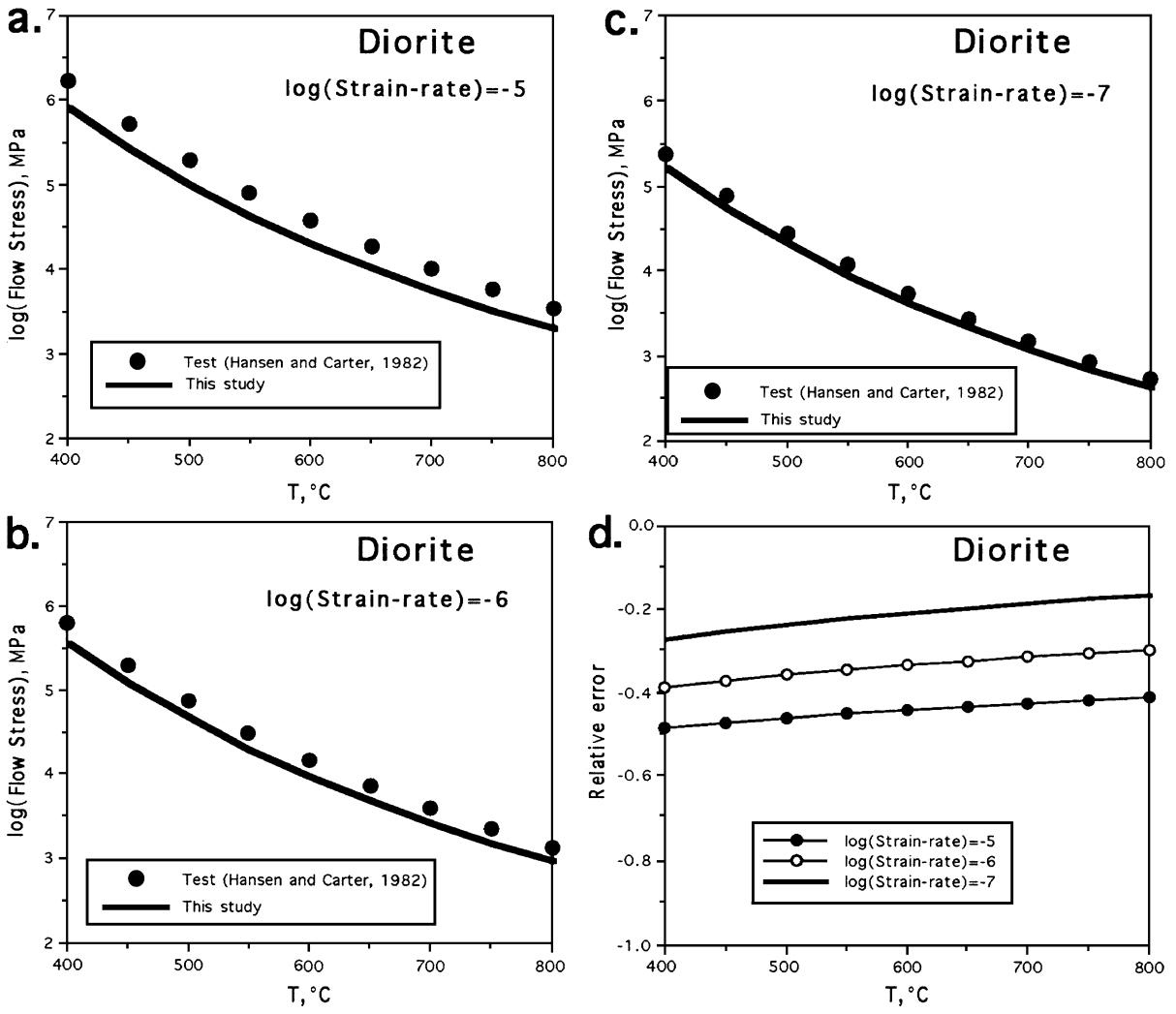

Fig. 2. Flow stress–temperature profiles for diorite at three different strain-rates of (a) 10^{-5}/s, (b) 10^{-6}/s and (c) 10^{-7}/s. (d) Relative error as a function of temperature. Experimental data from Hansen and Carter (1982).

of the polyphase rocks were judicially selected from the existing experimental data based on the following criteria:

1. Polyphase rocks and their constituent phases are experimentally determined under similar laboratory conditions because rheological data of both monophase aggregates and polyphase rocks are strongly dependent on the experimental conditions, such as temperature, strain-rate, confining pressure, water content, and test apparatus used. Strain-rate and temperature may play a more important role than confining pressure. When more than one set of experimental results satisfy this condition, results obtained from liquid and gas confining medium apparatus are regarded as most reliable and dry tests in a rocksalt confining medium in solid pressure medium equipment are next most reliable, but results from other solid pressure medium apparatus are less reliable (Carter and Tsenn, 1987).
2. The experimental results obtained from liquid or gas confining medium apparatus are regarded as

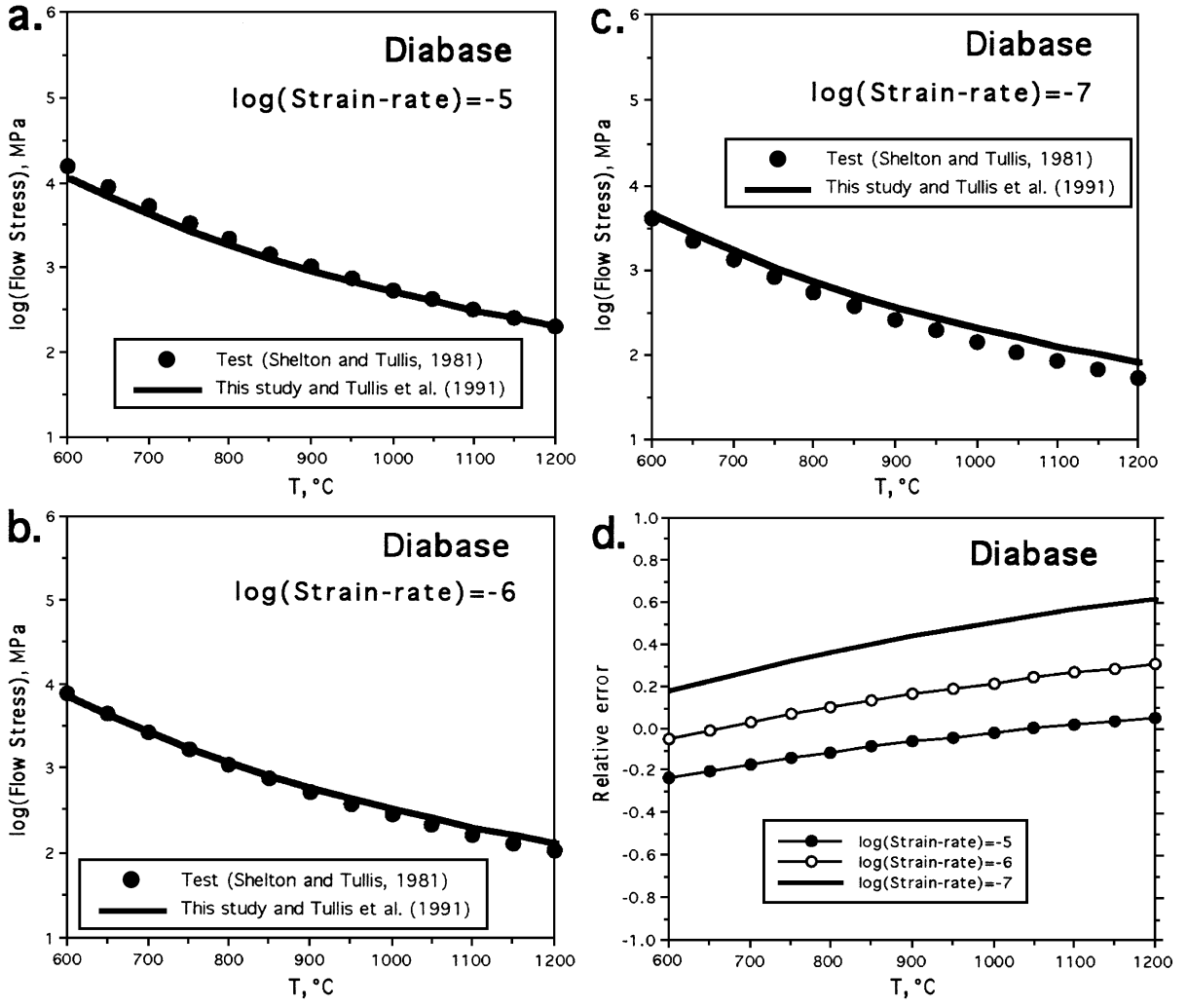

Fig. 3. Flow stress–temperature profiles for diabase at three different strain-rates of (a) 10^{-5}/s, (b) 10^{-6}/s and (c) 10^{-7}/s. (d) Relative error as a function of temperature. Experimental data from Shelton and Tullis (1981).

the remedial choice when there are no experimental results, which can satisfy the first selective criterion.

3. The deformed polyphase rocks are coarse and nearly equant-grained (≥ 5 μm), homogeneously mixed, dense aggregates.

If there is no experimental data for one or some of the constituent phases satisfying either of the above criteria, the comparison for such polyphase aggregates cannot be done unless there are experimental results of other monophase aggregates which satisfy either of the first two criteria to replace the constituent phases. For example, although flow law parameters of K-feldspar monophase aggregate are not available, they can be approximated by those of albite, because optical and transmission electron microscopy observations indicate that the deformation microstructures are almost identical for plagioclase and K-feldspar coexisting in naturally deformed granite (White and Mawer, 1986). Moreover, hornblende appears to display similar rheological properties to clinopyroxene.

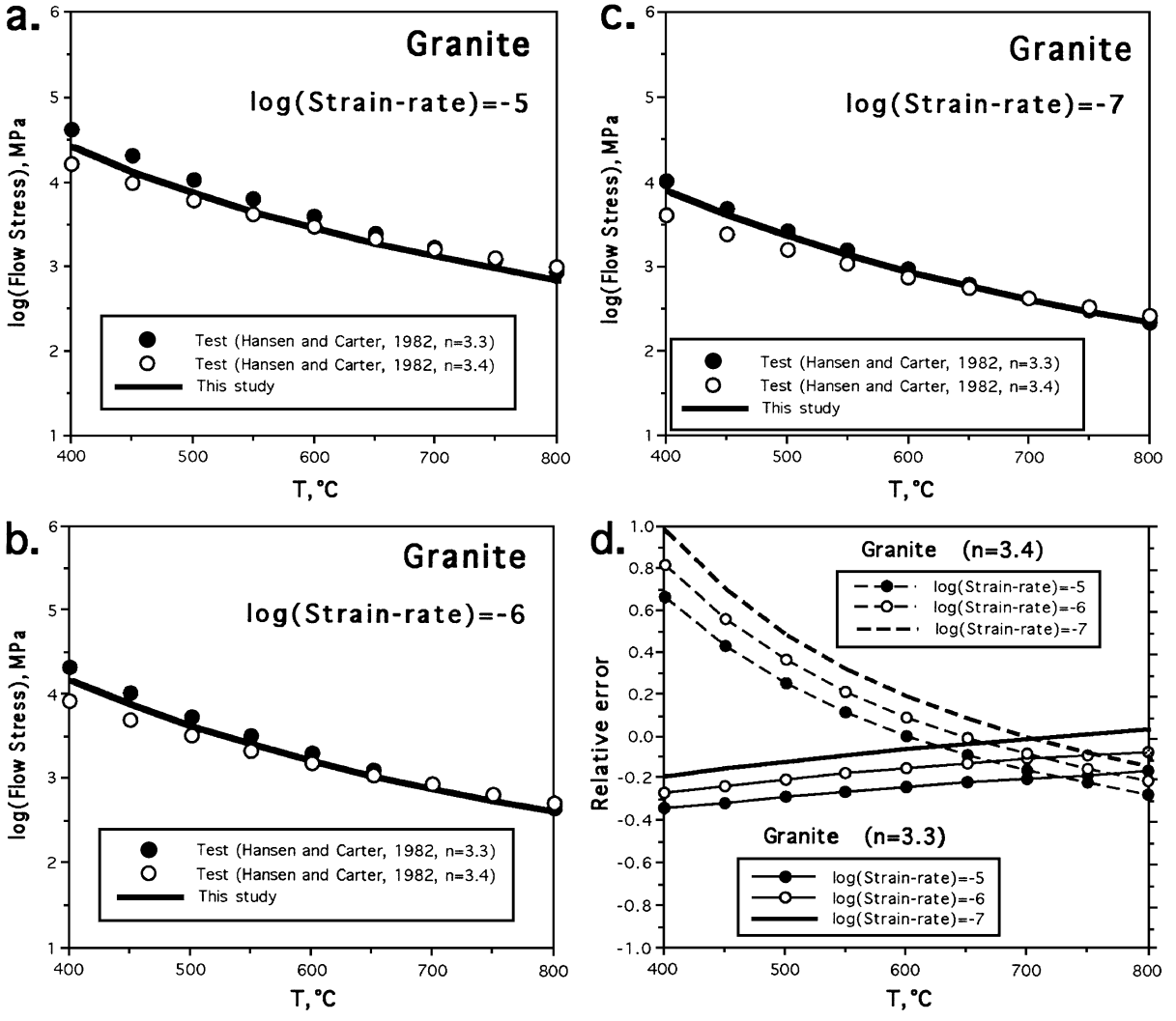

Fig. 4. Flow stress–temperature profiles for granite at three different strain-rates of (a) 10^{-5}/s, (b) 10^{-6}/s and (c) 10^{-7}/s. (d) Relative error as a function of temperature. Experimental data from Hansen and Carter (1982).

Comparisons are made between the predicted flow stresses (σ_p) and experimentally determined values (σ_e) as functions of temperature at different strain-rates for diorite (Fig. 2), diabase (Fig. 3), granite (Fig. 4), aplite (Fig. 5) and websterite (Fig. 6). At the experimental conditions, the constituent phases of these rocks were deformed mainly in the regime of dislocation creep, and the polyphase rocks obeyed the same kind of power flow laws as their constituent phases (Hansen and Carter, 1982; Shelton and Tullis, 1981; Kirby and Kronenberg, 1984; Shea and Kronenberg, 1992; Raleigh et al., 1971; Avé Lallemant, 1978). The contribution of the uniform stress condition and the uniform strain-rate condition are assumed to be the same, that is, $F=0.5$, in the iterative process. The precision (B) is taken to be 1%. The predicted flow stresses are quite close to those measured experimentally under the laboratory conditions, although the predicted flow law parameters for them may be different to some degree from those determined (Table 1). The relative errors $(\sigma_p-\sigma_e)/\sigma_e$ within the experimental temperature ranges are less than 0.7 except for granite. In the range of deformation temperature (e.g., 650–800 °C for diorite, 800–1100 °C for diabase,

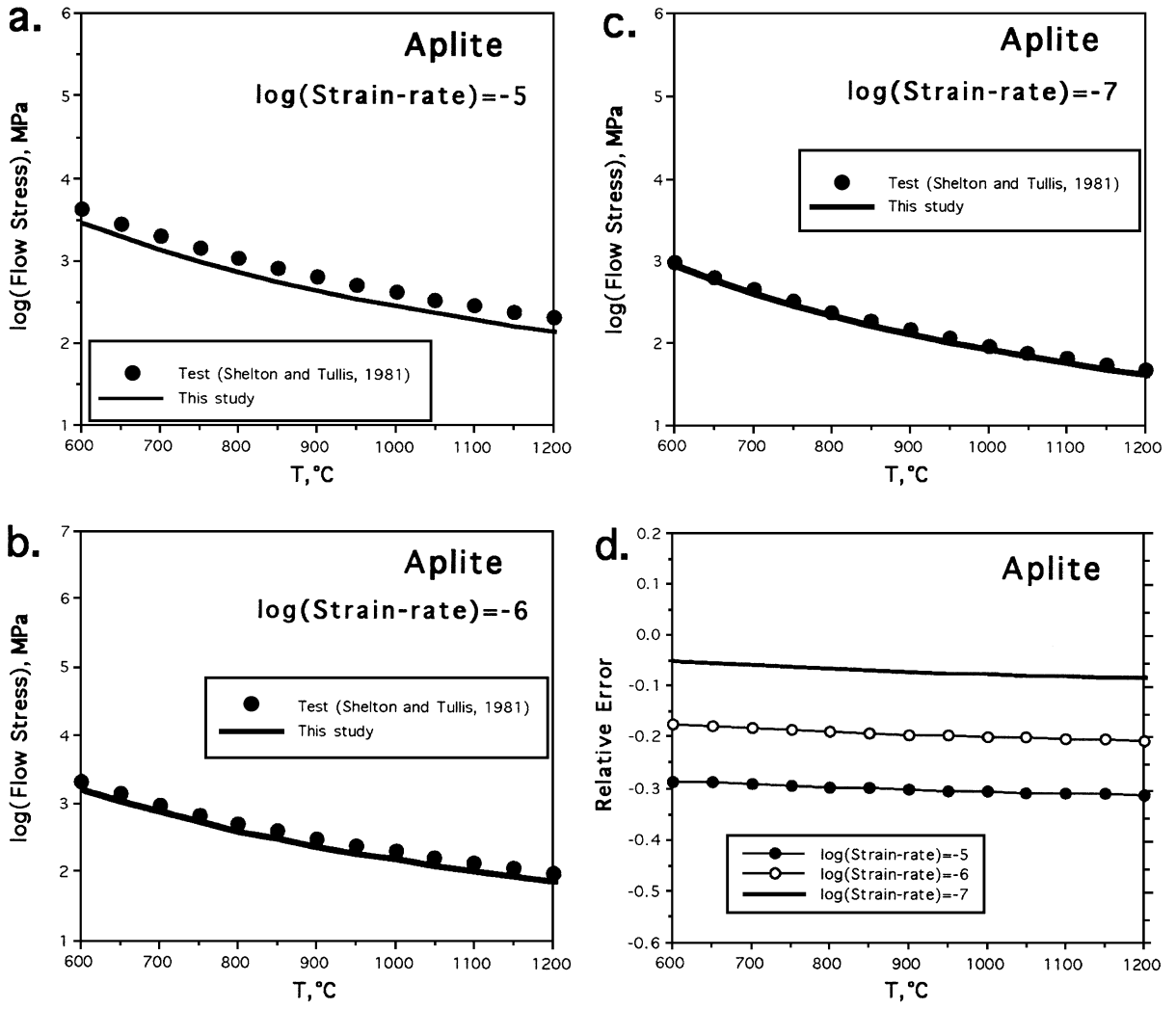

Fig. 5. Flow stress–temperature profiles for aplite at three different strain-rates of (a) 10^{-5}/s, (b) 10^{-6}/s and (c) 10^{-7}/s. (d) Relative error as a function of temperature. Experimental data from Shelton and Tullis (1981).

650–800 °C for granite, and 650–1125 °C for aplite), the relative errors are generally less than 0.53. The relative error varies from −0.42 to −0.18 for diorite (Fig. 2d), from −0.2 to 0.53 for diabase (Fig. 3d), from −0.29 to 0.1 for granite (Fig. 4d) and from −0.3 to −0.05 for aplite (Fig. 5d). The experimentally measured flow stress is larger than the predicted one for websterite (Fig. 6a–c). The relative error varies from −0.5 to −0.7 (Fig. 6d). Such errors may be due either to uncertainties in the input flow laws (Paterson, 1987) or to those in the model (e.g., effects of microstructures).

Recently, Ji et al. (2001) carried out a series of creep experiments to investigate the effect of varying forsterite content (V_{Fo}) on the bulk flow strength of dry forsterite–enstatite (Fo–En) aggregates. Their experiments were performed at temperatures of 1150–1320 °C, stresses of 18–100 MPa, oxygen fugacities of 10^{-14}–$10^{-2.5}$ MPa and 0.1 MPa total pressure. The fine-grained (Fo: 10–17 μm; En: 14–31 μm) composites of various Fo volume fractions (V_{Fo}=0, 0.2, 0.4, 0.5, 0.6, 0.8 and 1) were synthesized by isostatically hot-pressing in a gas medium apparatus at 1523 and 350 MPa. These experiments

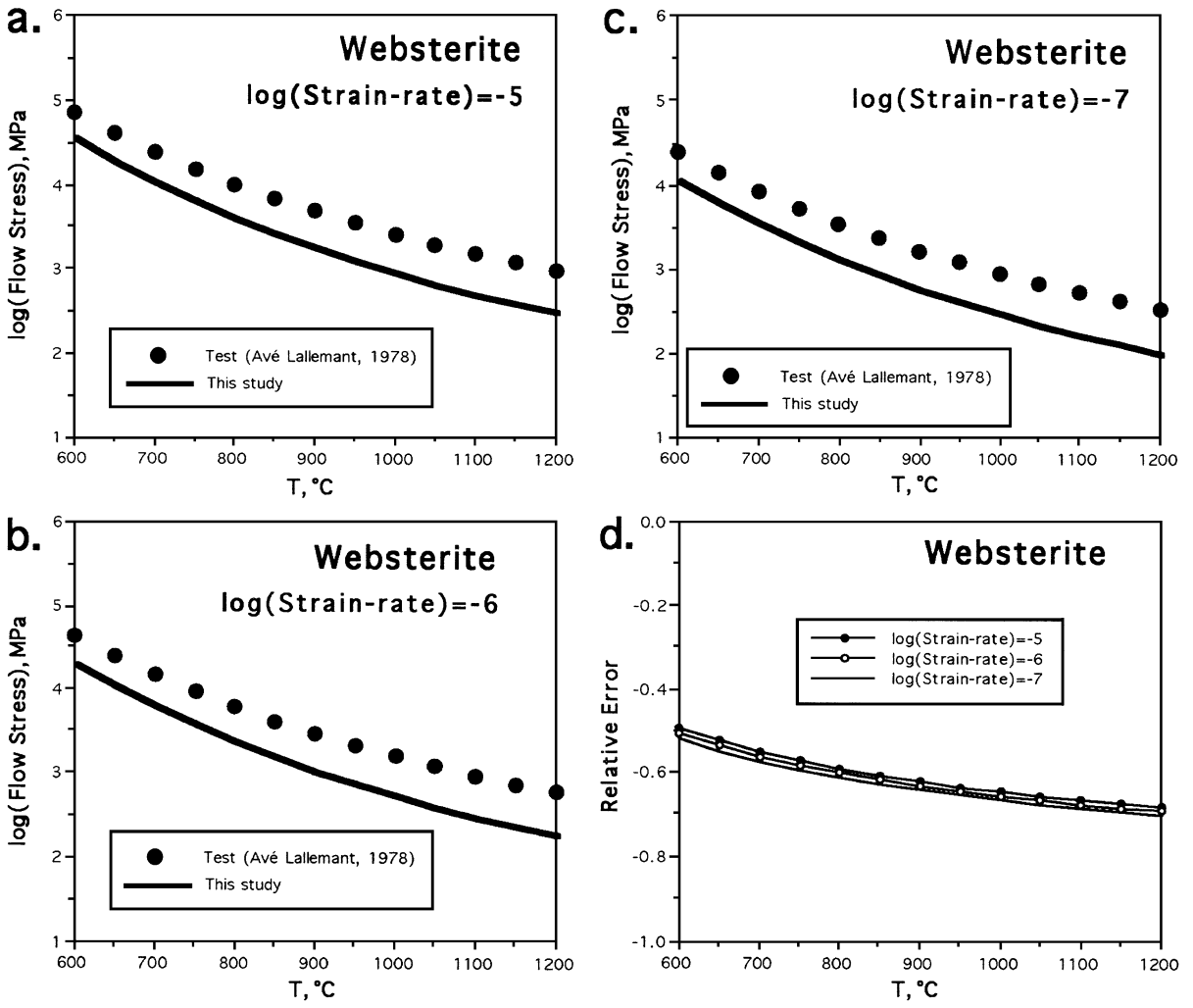

Fig. 6. Flow stress–temperature profiles for websterite at three different strain-rates of (a) 10^{-5}/s, (b) 10^{-6}/s and (c) 10^{-7}/s. (d) Relative error as a function of temperature. Experimental data from Avé Lallemant (1978).

show that flow strength contrasts between Fo and En are in the range of 3–8 at the given experimental conditions, with Fo as the stronger phase. The measured stress exponent (n) and activation energy (Q) values of the Fo–En composites fall between those of the end-members. The n values show a continuous increase from 1.3 to 2.0 while the Q values display a non-linear increase from 472 to 584 kJ/mol with En volume fraction from 0 to 1.0. The mechanical data and TEM microstructural observations suggest no change in deformation mechanism of each phase when in the composites, compared to when in a single phase aggregate. The En deformed mainly by dislocation creep while the Fo deformed mainly by diffusion creep for the grain sizes and experimental conditions. Fig. 7 shows the normalized flow stress as function of strong phase (forsterite) volume fraction for forsterite–enstatite (Fo–En) aggregates. The normalized flow stress (σ_N) is defined as

$$\sigma_N = \frac{\sigma_c - \sigma_w}{\sigma_s - \sigma_w} \tag{59}$$

where σ_w and σ_s are the flow stresses of the weaker phase and stronger phase, respectively. As shown in Fig. 7, the uniform stress and uniform strain-rate averages given by the present model are good approximations for the flow strengths of Fo–En composites with $V_{Fo} \leq 0.4$ and $V_{Fo} \geq 0.6$, respectively. At $V_{Fo} = 0.5$, the iteration with $F = 0.5$ predicts composite flow strengths consistent with the experimental data.

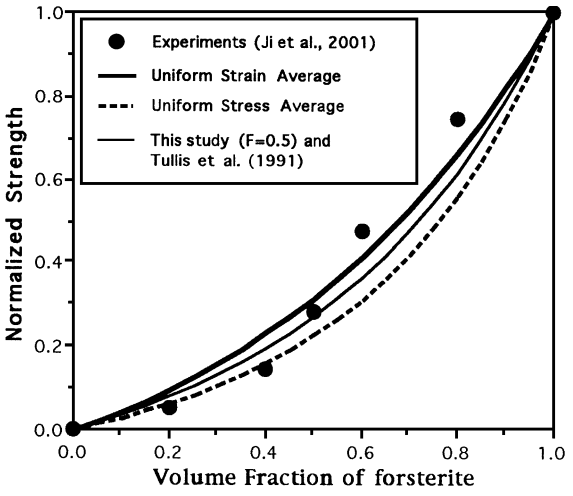

Fig. 7. Normalized flow stresses of hot-pressed forsterite–enstatite (Fo–En) aggregates at a strain rate of 10^{-6} s^{-1}, $T = 1230$ °C as a function of volume fraction of forsterite. Experimental data from Ji et al. (2001).

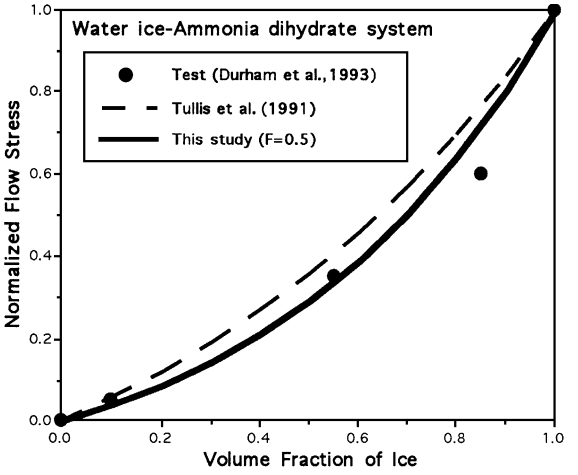

Fig. 8. Normalized flow stresses of water ice–ammonia alloys at a temperature of −97 °C and a strain-rate of 3.5×10^{-6}/s as a function of volume fraction of water ice. Experimental data from Durham et al. (1993).

Fig. 8 shows the normalized flow stress as function of strong phase volume fraction for water ice–ammonia dehydrate composites (Durham et al., 1993). At a temperature of 97 °C, a strain-rate 3.5×10^{-6}/s and a confining pressure 50 MPa, ice is stronger than ammonia and both phases deform by dislocation creep as indicated by high values of stress exponents (Table 2). The predicted flow stress values are in good agreement with those experimentally measured values under the experimental conditions. Both the predicted flow stresses (Fig. 8) and flow law parameters (Table 2) change with increasing the volume fraction of water ice.

It is interesting to compare the present model with the empirical formulas of Tullis et al. (1991). For a two-phase aggregate deformed by dislocation creep, Tullis et al. (1991) assumed

$$\log n_c = V_s \log n_s + V_w \log n_w \tag{60}$$

Table 2
Predicted flow parameters of water ice–ammonia dihydrate system

Volume fraction of ice (%)	A (MPa^{-n}/s)	n	Q (kJ/mol)
0	3.548×10^{21}	5.81	107.5
10	1.646×10^{19}	5.789	100.94
	(2.31×10^{19})	(5.789)	(100.9)
20	7.792×10^{16}	5.767	94.408
	(1.529×10^{17})	(5.767)	(94.408)
30	3.764×10^{14}	5.746	87.90
	(1.032×10^{15})	(5.746)	(87.90)
40	1.855×10^{12}	5.725	81.414
	(7.092×10^{12})	(5.725)	(81.415)
50	9.32×10^{9}	5.704	74.953
	(4.965×10^{10})	(5.704)	(74.953)
60	4.775×10^{7}	5.683	68.516
	(3.54×10^{8})	(5.683)	(68.515)
70	2.494×10^{5}	5.662	62.103
	(2.57×10^{6})	(5.662)	(62.101)
80	1.328×10^{3}	5.64	55.712
	(1.9×10^{4})	(5.641)	(55.711)
90	7.203	5.62	49.345
	(1.43×10^{2})	(5.621)	(49.344)
100	3.98×10^{-2}	5.6	43

The flow law parameters in the parentheses are predicted using the empirical formulas of Tullis et al. (1991).

Then based on this assumption, they obtained the flow law parameters Q_c and A_c of the composite from the following equations:

$$Q_c = \frac{Q_w(n_c - n_s) - Q_s(n_c - n_w)}{n_w - n_s} \tag{61}$$

$$A_c = 10^{\frac{\log A_w(n_c - n_s) - \log A_s(n_c - n_w)}{n_w - n_s}} \tag{62}$$

where the subscripts s and w stand for the strong phase and the weak phase, respectively. They found that the results calculated from Eqs. (60)–(62) agreed quite well with their finite element model calculations. As shown in Table 1, the stress exponents and the activation energies of diabase and websterite calculated from the empirical formulas of Tullis et al. (1991) are almost the same as those predicted by our model using $F = 0.5$. But the pre-exponential factors (A values) predicted from these two models are slightly different for these two bi-phase composite rocks. However, there is no remarkable difference in the calculated flow stresses between the two models for diabase (Fig. 3), websterite (Fig. 6) and forsterite–enstatite mixtures (Fig. 7). For ice–ammonia dehydrate system (Durham et al., 1993), the normalized flow stress predicted by our model (Fig. 8) is even closer to the experimental results than that predicted by the empirical formulas of Tullis et al. (1991). Furthermore, their empirical formulas are limited to only two-phase aggregates with $n_s \neq n_w$ while the present model can be easily applied for any multiphase rocks.

6. Discussion and conclusions

The iterative process presented in this paper allows prediction of the flow law parameters of polyphase materials and rocks in terms of the flow law parameters and volume fractions of their constituent phases, no matter whether each of the phases deforms by dislocation creep or diffusion creep, as long as there is no change in deformation mechanism when it is in the composites as compared to when it is in a monophase aggregate. Although the predicted flow law parameters may be different to some degree from those experimentally determined, the flow stresses calculated by the model are in good agreement with those measured experimentally under the laboratory conditions. Unlike most of the previous models which were developed for modeling the bulk flow strength of two-phase mixtures (e.g., Tharp, 1983; Duva, 1984; Tullis et al., 1991; Ji and Zhao, 1994; Handy, 1994; Takeda, 1998; Treagus, 2002), the present model can be used to predict the flow law parameters of multiphase aggregates. For two-phase aggregates, the flow strengths estimated by our model using $F = 0.5$ are almost the same as calculated by the empirical formulas of Tullis et al. (1991) for two-phase aggregates such as diabase, websterite and forsterite–enstatite mixtures.

Although the analysis presented in Section 2 of this paper is derived for the generalized power flow law described by Eq. (1), the comparisons with experimental results are mainly limited to the dislocation-creep power laws which are independent on the grain size ($m = 0$), because so far, most of the experimental data were obtained from the regime of dislocation creep. Even in the diffusion creep regime, grain size exponent is generally difficult to determine

because the mean grain sizes of the samples should vary in such a large range that the grain size exponent can be well constrained (Walker et al., 1990). We believe that our model is valid for the polyphase materials and rocks in which each of the constituent phases deforms in the same mechanism as in its monophase aggregate. Thus, the model cannot be applied to the polyphase composites in which the operative deformation mechanisms are different from those in the end-member aggregates (Wheeler, 1992; Bruhn et al., 1999), chemical or metamorphic reactions take place among the constituent phases (Brodie and Rutter, 1985), or eutectic melting occurs due to phase mixing (e.g., Rutter and Neumann, 1995). Further testing of the proposed model will require systemic, carefully designed experiments on synthetic homogeneous aggregates of controlled composition, grain size, volume fraction and microstructure of each phase.

The model is also extended to predict the exponential law parameters for polyphase aggregates when all of their constituent phases obey the exponential laws. Unfortunately, the proposed model cannot be used to estimate the flow properties of polyphase aggregates when their constituent phases obey different types of flow laws, for example, some phases obey power laws while the others obey exponential laws.

The model developed in this paper is appropriate only for the coarse (≥ 5 μm), nearly equant-grained (aspect-ratio ≤ 3), and massive materials because of neglecting the possible contribution of microstructures to the composite flow strength. For example, extremely fine-grained (<2 μm) hard phases can act as impenetrable barriers to dislocation motion in their soft matrix, and consequently increase the bulk flow strength of the polyphase aggregate (Kelley, 1973). The bulk flow strength of a polyphase material with constant volume fractions of constituents varies with the shape of the strong phase grains and increases with increasing the aspect-ratio of hard phases (Dragone and Nix, 1990; Ji and Zhao, 1994; Ji et al., 2000; Treagus, 2002). Furthermore, the phase continuity and interconnectivity play an important role in the rheological behavior of polyphase materials (Burg and Wilson, 1987; Jordan, 1988; Handy, 1990). A drastic decrease in bulk flow strength may occur in two-phase systems with contrasting rheology when a transition from strong-phase supported structure to weak-phase supported structure takes place (Arzi, 1978; Rutter and Neumann, 1995; Ji et al., 2001). Obviously, the influences of microstructures on the bulk rheology of polyphase materials are extremely complex, so far still poorly understood, and thus need further systematic investigation.

In spite of the above limitations, the model offers a first approximation for calculating flow strengths and flow law parameters of polyphase materials and rocks from their end-member flow laws and modal compositions. Thus, it is a useful approach for predicting the flow laws of a large number of rocks based on the experimentally determined flow laws of a relatively small number of monophase aggregates.

Acknowledgements

We thank the NSERC and LITHOPROBE of Canada for research grants. Dr. E. Rutter and two anonymous reviewers are thanked for thoughtfully reviewing the manuscript. This is LITHOPROBE contribution No. 1281.

References

Arzi, A.A., 1978. Critical phenomena in the rheology of partially melted rocks. Tectonophysics 44, 173–184.

Avé Lallemant, H.G., 1978. Experimental deformation of diopside and websterite. Tectonophysics 48, 1–27.

Bloomfield, J.P., Covey-Crump, J., 1993. Correlating mechanical data with microstructural observations in deformation experiments on synthetic two-phase aggregates. J. Struct. Geol. 15, 1007–1019.

Brodie, K., Rutter, E.H., 1985. On the relationship between deformation and metamorphism with special reference to the behavior of basic rocks. In: Thompson, A.B., Rubie, D. (Eds.), Kinetics, Textures and Deformation. Adv. Phys. Geochem., vol. 4. Springer-Verlag, New York, pp. 138–179.

Bruhn, D.F., Olgaard, D.L., Dell'Angelo, L.N., 1999. Evidence for enhanced deformation in two-phase rocks: experiments on the rheology of calcite–anhydrite aggregates. J. Geophys. Res. 104, 707–724.

Burg, J.P., Wilson, C.J.L., 1987. Deformation of two-phase systems with contrasting rheology. Tectonophysics 135, 199–205.

Carter, N.L., Tsenn, M.C., 1987. Flow properties of continental lithosphere. Tectonophysics 136, 27–63.

Dragone, T.L., Nix, W.D., 1990. Geometric factors affecting the internal stress distribution and high temperature creep rate of

discontinuous fiber reinforced metals. Acta Metall. Mater. 38, 1941–1953.

Dresen, G., Evans, B., Olgaard, D.L., 1998. Effect of quartz inclusions on plastic flow in marble. Geophys. Res. Lett. 25, 1245–1248.

Durham, W.B., Kirby, S.H., Stern, L.A., 1993. Flow of ices in the ammonia–water system. J. Geophys. Res. 98 (B10), 17667–17682.

Duva, J.M., 1984. A self-consistent analysis of the stiffening effect of rigid inclusions on a power-law material. J. Eng. Mater. Technol. 106, 317–321.

Handy, M.R., 1990. The solid-state flow of polymineralic rocks (the corrected form). J. Geophys. Res. 95, 8647–8661.

Handy, M.R., 1994. Flow laws for rocks containing two non-linear viscous phases: a phenomenological approach (the corrected form). J. Struct. Geol. 16, 287–301.

Hansen, F.D., Carter, N.L., 1982. Creep of selected crustal rocks at 1000 MPa. Eos. Trans. Am. Geophys. Union 63, 437.

Ji, S.C., Wang, Z.C., 1999. Elastic properties of forsterite–enstatite composites up to 3.0 GPa. J. Geodyn. 28, 147–174.

Ji, S.C., Zhao, P.L., 1993. Flow laws of multiphase rocks calculated from experimental data on the constituent phases. Earth Planet. Sci. Lett. 117, 181–187.

Ji, S.C., Zhao, P.L., 1994. Strength of two-phase rocks: a model based on fiber-loading theory. J. Struct. Geol. 16, 253–262.

Ji, S.C., Wirth, R., Rybacki, E., Jiang, Z.T., 2000. High temperature plastic deformation of quartz–plagioclase multilayers by layer-normal compression. J. Geophys. Res. 105 (B7), 16651–16664.

Ji, S.C., Wang, Z.C., Wirth, R., 2001. Bulk flow strength of forsterite–enstatite composites as a function of forsterite content. Tectonophysics 341, 69–93.

Jordan, P., 1988. The rheology of polymineralic rocks: an approach. Geol. Rundsch. 77, 285–294.

Karato, S., Paterson, M.S., Fitz Gerald, J.D., 1986. Rheology of synthetic olivine aggregates: influence of grain-size and water. J. Geophys. Res. 91, 8151–8176.

Kelley, P.M., 1973. The quantitative relationship between microstructure and properties in two-phase alloys. Int. Metall. Rev. 18, 31–36.

Kelly, A., Macmillan, N.H., 1986. Strong Solids. Oxford Science Publications, Oxford. 423 pp.

Kirby, S.H., Kronenberg, A., 1984. Deformation of clinopyroxenite: evidence for a transition in flow mechanisms and semibrittle behavior. J. Geophys. Res. 89, 3177–3192.

Kohlstedt, D.L., Evans, B., Mackwell, S.J., 1995. Strength of the lithosphere: constraints imposed by laboratory experiments. J. Geophys. Res. 100, 17587–17602.

Mackwell, S.J., Zimmermann, M.E., Kohlstedt, D.L., 1998. High temperature deformation of dry diabase with application to tectonics on Venus. J. Geophys. Res. 103, 975–984.

McDonnell, R.D., Peach, C.J., van Roermund, H.L.M., Spiers, C.J., 2000. Effect of varying enstatite content on the deformation behavior of fine-grained synthetic peridotite under wet conditions. J. Geophys. Res. 105, 13535–13553.

Park, Y.H., Holmes, J.W., 1992. Finite element modelling of creep deformation in fibre-reinforced ceramic composites. J. Mater. Sci. 27, 6341–6351.

Paterson, M.S., 1987. Problems in the extrapolation of laboratory rheological data. Tectonophysics 133, 33–43.

Poirier, J.P., 1985. Creep of Crystals. Cambridge Univ. Press, New York, p. 260.

Raleigh, C.B., Kirby, S.H., Carter, N.L., Avé Lallemant, H.G., 1971. Slip and the clinoenstatite transformation as competing rate processes in enstatite. J. Geophys. Res. 76 (17), 4011–4022.

Reuss, A., 1929. Berechnung der Fliessgrenze von Mischkristallen auf Grund der Plastizitätsbedingung für Einkristalle. Z. Angew. Math. Mech. 9, 49–58.

Ross, J.V., Bauer, S.J., Hansen, F.D., 1987. Texture evolution of synthetic anhydrite–halite mylonite. Tectonophysics 140, 307–326.

Rutter, E.H., 1976. The kinetics of rock deformation by pressure solution. Philos. Trans. R. Soc. Lond., A 283, 203–219.

Rutter, E.H., Brodie, K.H., 1992. Rheology of the lower crust. In: Fountain, D.M., Arculus, R., Kay, R.W. (Eds.), Continental Lower Crust. Elsevier, New York, pp. 201–267.

Rutter, E.H., Neumann, D.H.K., 1995. Experimental deformation of partially molten Westerly granite under fluid-absent conditions, with implications for the extraction of granitic magma. J. Geophys. Res. 100, 15697–15715.

Rybacki, E., Dresen, G., 2000. Dislocation and diffusion creep of synthetic anorthite aggregates. J. Geophys. Res. 105, 26017–26036.

Shea, W.T., Kronenberg, A.K., 1992. Rheology and deformation mechanisms of an isotropic mica schist. J. Geophys. Res. 97 (B11), 15201–15237.

Shelton, G.L., Tullis, J., 1981. Experimental flow laws for crustal rocks. Eos. Trans. Am. Geophys. Union 62, 396.

Sherby, O.D., Ord, R.L., Dorn, J.E., 1954. Creep corrections of metals at elevated temperatures. Trans. AIME 200, 71–81.

Takeda, Y.T., 1998. Flow in rocks modeled as multiphase continua: application to polymineralic rocks. J. Struct. Geol. 20, 1569–1578.

Tharp, T.M., 1983. Analogies between the high-temperature deformation of polyphase rocks and the mechanical behavior of porous powder metal. Tectonophysics 96, T1–T11.

Treagus, S.H., 2002. Modelling the bulk viscosity of two-phase mixtures in terms of clast shape. J. Struct. Geol. 24, 57–76.

Tsenn, M.C., Carter, N.L., 1987. Upper limits of power law creep of rocks. Tectonophysics 136, 1–26.

Tullis, J., Wenk, H.R., 1994. Effect of muscovite on the strength and lattice preferred orientations of experimentally deformed quartz aggregates. Mater. Sci. Eng., A 175, 209–220.

Tullis, T.E., Horowitz, F.G., Tullis, J., 1991. Flow laws of polyphase aggregates from end-member flow laws. J. Geophys. Res. 96 (B5), 8081–8096.

Voigt, W., 1928. Lehrbuch der Kristallphysik. Teubner, Leipzig.

Walker, A.N., Rutter, E.H., Brodie, K.H., 1990. Experimental study of grain-size sensitive flow of synthetic, hot-pressed calcite rock. In: Knipe, R.J., Rutter, E.H. (Eds.), Deformation Mechanisms, Rheology and Tectonics. Special Publication, vol. 54. Geological Society, London, pp. 259–284.

Wang, J.N., 1994. The effect of grain size distribution on the rheological behavior of polycrystalline materials. J. Struct. Geol. 16, 961–970.

Watt, J.P., Davies, G.F., O'Connell, R.J., 1976. The elastic properties of composite materials. J. Geophys. Res. 14, 541–563.
Wheeler, J., 1992. Importance of pressure solution and Coble creep in the deformation of polymineralic rocks. J. Geophys. Res. 97, 4586–4597.
White, J.C., Mawer, C.K., 1986. Extreme ductility of feldspars from a mylonite, Parry Sound, Canada. J. Struct. Geol. 8, 133–143.
Zhao, P.L., Ji, S.C., 1997. Refinements of shear-lag model and its applications. Tectonophysics 279, 37–53.